Matrix Biology 143 (2026) 1–13

Contents lists available at ScienceDirect

Matrix Biology

journal homepage: www.elsevier.com/locate/matbio

Furin-like cleavage at the C1-C2 linker region of the α3 chain is not required for collagen VI assembly

Arthur Lauri Pasanen-Zentz [a,1], Mengjie Zhu [a,1], Sebastian Schmitz [a], Nitin George Eapen [c], Matthias Pzryklenk [a], Fabian Metzen [a], Karina Hadrian [d,e], Matthias Mörgelin [f], Uwe Hansen [g], Branko Zevnik [c,h], Simon E Tröder [c,h], Felix Bock [d,e], Catherine Moali [i], Marcus Krüger [b,c], Manuel Koch [a,j], Mats Paulsson [a,e], Raimund Wagener [a], Alvise Schiavinato [a,e,k,*]

[a] Center for Biochemistry, Medical Faculty, University of Cologne, Cologne, Germany
[b] Institute for Genetics, Cologne Excellence Cluster for Aging and Aging-Associated Diseases (CECAD), University of Cologne, Cologne, Germany
[c] Cluster of Excellence Cellular Stress Responses in Aging-Associated Diseases (CECAD), Faculty of Medicine and University Hospital Cologne, University of Cologne, Cologne, Germany
[d] Translational Experimental Ophthalmology Cologne (TEO-C), University Hospital of Cologne, Germany
[e] Center for Molecular Medicine Cologne (CMMC), University of Cologne, Germany
[f] Colzyx AB, Medicon Village, Lund, Sweden
[g] Institute of Musculoskeletal Medicine, University Hospital Munster, Munster, Germany
[h] In Vivo Research Facility, Faculty of Medicine and University Hospital Cologne, University of Cologne, Cologne, Germany
[i] Université Claude Bernard Lyon 1, CNRS, Tissue Biology and Therapeutic Engineering Laboratory, LBTI, Lyon, France
[j] Institute for Dental Research and Oral Musculoskeletal Biology, Faculty of Medicine and University Hospital Cologne, University of Cologne, Cologne, Germany
[k] Department of Pediatrics and Adolescent Medicine, Faculty of Medicine and University Hospital Cologne, Cologne, Germany

ARTICLE INFO

Keywords:
Collagen VI
Proprotein convertases
Furin
Endotrophin

ABSTRACT

Collagen VI is a heterotrimeric, ubiquitously expressed microfibrillar collagen with a complex intracellular and extracellular assembly process. In addition to a short collagenous region, it is primarily composed of von Willebrand factor A (VWA) domains. Notably, only the C-terminal end of the α3 chain contains other domain types, including a Kunitz-like C5 domain, which has been reported to be necessary for microfibril formation, to function as a matrikine and exhibit biomarker properties. This region of the α3 chain undergoes proteolytic processing, with cleavage sites identified for proprotein convertases, matrix metalloproteinases (MMPs), and bone morphogenetic protein 1 (BMP1). Cleavage by furin-like convertases results in the generation of a mature collagen VI α3 chain lacking its 70 kDa C2-C5 domains. Here, we provide the first characterization of the functional significance of the furin-like cleavage site, demonstrating that while it is constitutively used, it is not essential for collagen VI assembly, microfibril formation, or skeletal muscle function under physiological conditions, likely due to the presence of redundant cleavage sites. We also present an initial characterization of the biological activity of the released fragments on myoblast cultures showing that they do not affect C2C12 myoblast behaviour or differentiation. These findings deepen our understanding of α3 chain processing and highlight its potential significance for collagen VI assembly and function, including the generation of peptides with potential biomarker and biological activity properties.

Introduction

Collagen VI microfibrils are abundant in most tissues and closely associated with basement membranes in nerves, blood vessels or muscle and anchor these to the surrounding extracellular matrix [1]. The major collagen VI isoform consists of three different α chains, two shorter α1 and α2 and a longer α3 chain. Mutations in *COL6A1, COL6A2* and *COL6A3* lead to muscular dystrophies and other myopathies [2]. Three

* Corresponding author at: Center for Biochemistry, Medical Faculty, University of Cologne, Cologne, Germany.
E-mail address: aschiav1@uni-koeln.de (A. Schiavinato).
[1] These authors contributed equally.

https://doi.org/10.1016/j.matbio.2025.11.003
Received 24 June 2025; Received in revised form 14 November 2025; Accepted 14 November 2025
Available online 15 November 2025

additional long α chains (α4, α5, α6) exist that can replace the α3 chain [3,4]. However, collagen VI assemblies containing the additional long chains have a very restricted tissue distribution [5].

The domain structure of collagen VI chains is unique within the collagen family. All α chains have only a short, about 340 amino acid residue long, collagenous stretch and more than 75 % of the structure consists of globular regions that are dominated by tandem arrays of VWA domains [6]. Such domains typically mediate adhesion to other proteins, often via metal ion dependent adhesion sites (MIDAS), and collagen VI has the highest relative content of VWA domains in the human proteome. In addition, other domains are present in the C-terminal part of all long chains [3,5]. Among those the 7 kDa C5 domain at the C-terminus of the collagen VI α3 chain, a Kunitz domain, attracted interest in recent years and a novel non-microfibril related function for the cleaved off C5 domain was proposed [7,8]. It is referred to as "endotrophin" and when released in white adipose tissue is assumed to act as an adipokine [9]. It was reported that it enhances breast tumor progression, increases fibrosis and inflammation and ultimately causes enhanced insulin resistance [10]. However, the acting mechanism remains to be obscure, in particular as no cellular receptor has been identified [11]. Moreover, recent studies proposed circulating levels of endotrophin-containing peptides as a predictive biomarker for various pathological conditions [12,13]. The assembly of collagen VI microfibrils is a complex multistep process including proteolytic processing at later steps [14]. A short α1 chain, a short α2 chain and a long chain, predominantly the α3 chain, form a heterotrimeric triple helical monomer, a process that was recently shown to depend only on a short coiled coil region C-terminal to the collagenous domain, and not on the C-terminal globular domains [15]. Two monomers form antiparallel dimers in which about 70 % of the collagenous domains adopt a twisted, segmented supercoil composed of two triple helices, while the most N-terminal part remains unconnected to the neighboring monomer within the dimer [16]. An interaction between C-terminal VWA domains and the collagenous domains is potentially important for dimer formation, however, the experimental evidence is not clear [17,18]. The dimers are stabilized by disulfide bonds between the monomers, but the exact localization of these is not known. The dimers then associate laterally and form tetramers that are also disulfide linked, but again the cysteine residues involved have not been determined. The fully assembled tetramers, large protein complexes of the size of ribosomes, are secreted and by partial interlocking of the globular domains assemble head-to-head to form the typical beaded microfibrils via non-covalent interactions [19,20].

The extracellular microfibril assembly is accompanied by extensive proteolytic cleavage within the C-terminal, non-collagenous part of the α3 chain. In fact, the Kunitz domain (C5) of the α3 chain is a prerequisite for microfibril formation [21], but mature collagen VI isolated from tissue lacks the whole 70 kDa C5-containing C2-C5 region of the α3 chain [22]. It was shown that BMP1 and MMP14 cleave C5 from the rest of the α3 chain, albeit by use of a different cleavage site, and furthermore a conserved furin-like proprotein convertase cleavage site between the C1 and C2 domains facilitates the cleavage of the large C2-C5 fragment [14,23]. For simplicity this cleavage site is here further named "furin-like cleavage site". In addition, more C5-containing fragments of different sizes were identified pointing to complex proteolytic processing within the C-terminal globular region of the collagen VI α3 chain [14]. However, the exact role of the proteolytic cleavage for the formation of functional collagen VI microfibrils remains to be elucidated. It is also not known if a perturbance of the processing is linked to the collagen VI related myopathies.

Using cell culture and a mouse model, we investigated the consequences of abolishing the furin-like cleavage site of the α3 chain between C1 and C2 on collagen VI assembly and function and studied the impact of the normally released C-terminal fragments on myoblast cultures.

Results

In vitro validation of the furin-like cleavage site in the C-terminal part of the collagen VI α3 chain

We previously identified a furin-like cleavage site (RDRR) in the C-terminal part of the collagen VI α3 chain, located in a linker region between the C1 and C2 domains (Fig. 1A) [14]. To confirm the role of the furin-like cleavage site in the proteolytic processing of the α3 chain, we mutated the cleavage site to RDAA (ΔFurin-α3 chain, Fig. 1B), expressed full-length wild type and mutated collagen VI α3 chains in HEK293 cells, and purified the respective protein products. Affinity purification using a tag placed at the C-terminus of the proteins revealed that the wild type protein is efficiently cleaved in the cell culture, releasing a fragment with an apparent molecular weight of about 110 kDa, presumably representing the C2-C5 portion at the C-terminal end of the α3 chain. Notably, this fragment was absent in the preparation of the mutant protein, indicating that cleavage at the furin-like site occurs with the monomeric α3 chain *in vitro* and that the introduced mutation effectively blocks cleavage. In-gel digestion coupled with mass spectrometry confirmed the identity of the recovered band as the C2-C5 fragment. Interestingly, also a smaller band, corresponding to the C5 domain, was recovered from both recombinant protein preparations (Fig. 1C).

Next, to test whether the furin-like cleavage site is required for collagen VI assembly or secretion *in vitro*, we generated HEK293 cells co-expressing α1 and α2 chains with either wild type or ΔFurin α3 chain. Both cell lines were able to assemble and secrete collagen VI tetramers with similar efficiency, indicating that furin-like-mediated processing of the α3 chain is not necessary for the assembly and secretion of collagen VI *in vitro* (Fig. 1D).

The α3 furin-like cleavage site is dispensable for collagen VI deposition in vivo

To investigate whether processing at the furin-like cleavage site plays a specific role in collagen VI microfibril assembly and to assess the *in vivo* significance of this site, we generated a mouse line carrying the same mutation (RDAA) using the CRISPR/Cas9 approach (see Materials and Methods). The mice were backcrossed onto a C57BL/6 N genetic background. Homozygous mutant mice (ΔFurin) were born at the expected Mendelian rate and did not exhibit any evident phenotype. Up to one year of age, they showed no macroscopic alterations and had a comparable weight to their wild type littermates (Supplementary Figure 1A-B). Collagen VI is a major extracellular matrix component of skeletal muscle, where it plays a critical role in maintaining tissue homeostasis, as demonstrated in collagen VI-related myopathies. To study microfibril deposition in muscle, we applied antibodies specific for different collagen VI epitopes to muscle sections (Fig. 2A-D). In both wild type and ΔFurin muscle, we observed the expected distribution pattern of collagen VI, with strong and uniform staining in the endomysium and perimysium, as revealed by the overlapping signals of antibodies directed against the N-terminal part of the α3(VI) chain and against the α1(VI) chain (Fig. 2A). Agarose–polyacrylamide composite gel analysis of protein extracts showed that both the α1 and α3 chains were assembled into collagen VI tetramers in both wild type and ΔFurin muscle (Supplementary Figure 2A). In the endomysium, collagen VI microfibrils are closely associated with the basement membrane, and this association is lost when collagen VI fails to assemble normally, as occurs with disease-causing mutations [24]. To investigate this, we performed colocalization studies of collagen VI with two basement membrane markers, collagen IV and nidogen-1, and observed similar colocalization patterns in both wild-type and ΔFurin muscle (Supplementary Figure 2B-C). We further probed the same muscle sections with the ER-TR7 antibody, which we previously identified as a conformation-dependent antibody against collagen VI [25], and

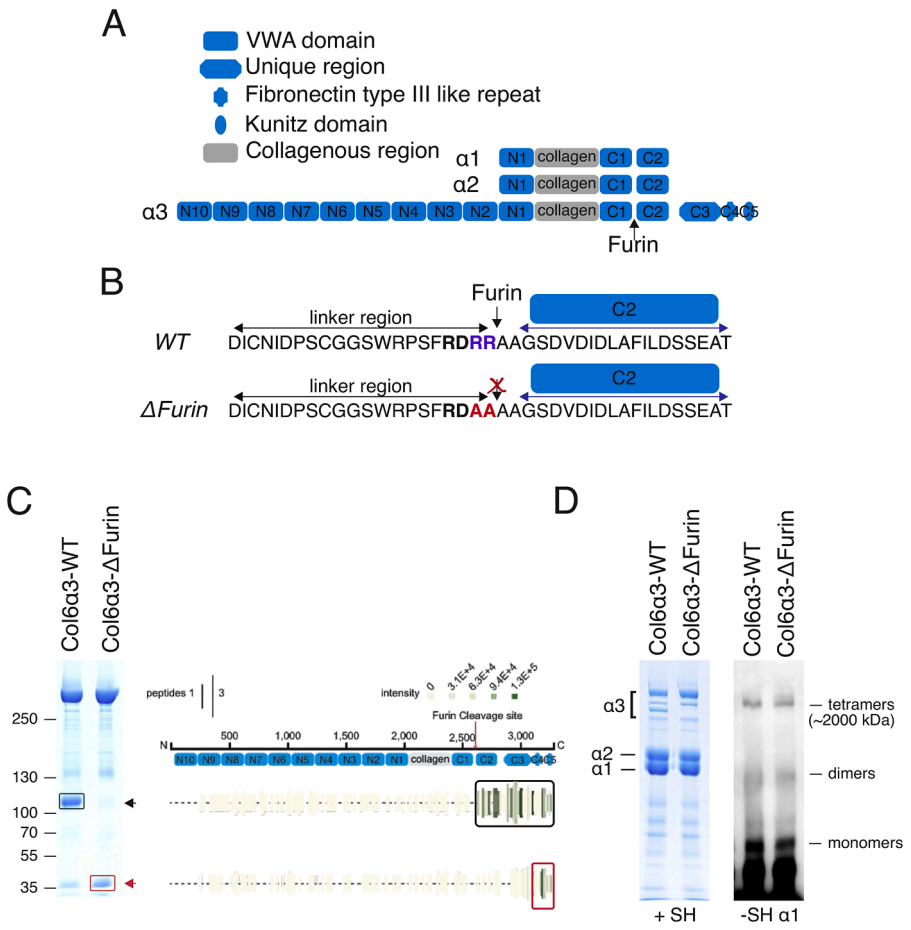

Fig. 1. The furin cleavage site is used in a recombinantly expressed collagen VI α3 chain, but it is not required for *in vitro* assembly and secretion of recombinant collagen VI tetramers. (A) Schematic representation of the structure and domain composition of collagen VI α1, α2 and α3 chains. The localization of the furin cleavage site in the α3 chain is marked by an arrow. (B) Schematic representation of the furin cleavage site and of the strategy used to generate a ΔFurin mutant α3 chain. (C) Coomassie stained polyacrylamide gel showing purified wild type and ΔFurin α3 chains produced in HEK293 cells. Note the presence of a band in the wild type but not ΔFurin protein corresponding to the fragment generated by the furin activity (*black arrow*). The peptidogram on the right side shows the intensities of the peptides that were recovered from the bands boxed (in *red* and *black*) on the gel. The domain structure of the α3 chain is shown on top of the peptidogram for reference. (D) HEK293 cells were stably co-transfected with constructs coding for murine α1, α2 and either wild type or ΔFurin α3 chains. Serum free culture media was analyzed by SDS-PAGE under reducing conditions (+ SH) followed by Coomassie staining to show the comparable expression of the three chains. On the right, the same media were analyzed on agarose/polyacrylamide composite gels under non reducing conditions (- SH) and immunoblotted with an α1-specific antibody to monitor the secretion of collagen VI multimers. Note that transfection of the ΔFurin α3 chain resulted in the formation of collagen VI multimers similar to the wild type condition.

detected identical signals in wild-type and ΔFurin samples (Supplementary Figure 2D). Together, these results indicate that abrogation of the furin-like cleavage site does not affect the microfibrillar organization of collagen VI in muscle. Additionally, co-staining with an antibody against the C-terminal region of the α3(VI) chain (C1-C5 domains) revealed a signal that largely overlapped with that of the α3N antibody, with consistent results across both wild type and ΔFurin muscles (Fig. 2B). Given the location of the furin-like cleavage site between the C1 and C2 domains of the α3 chain, we generated an antibody directed only against the C2 domain. Strikingly, staining of muscle sections with this antibody revealed almost no signal in wild type muscle, whereas in the ΔFurin background, a strong signal co-localizing with the α3N labeling was observed (Fig. 2C). Interestingly, the C5-specific antibody produced a relatively weak signal within the muscle interstitial extracellular matrix in both genotypes, indicating that this domain may not be incorporated into the deposited microfibrils. However, a distinctly stronger signal was observed at the intersection points of certain myofibers in both wildtype and ΔFurin muscle (Fig. 2D). These C5-positive signals appeared localized to the pericellular space of cells situated within the interstitial region, an area typically occupied by muscle fibroblasts. Supporting this, co-labeling with the quiescent satellite cell marker PAX7 revealed no overlap, indicating that the C5 signal does not likely originate from satellite cells (Supplementary Figure 3A and B) which confirmed earlier work [26]. Furthermore, co-labeling with the endothelial marker CD31 showed partial colocalization with C5, suggesting that newly synthesized collagen VI is at least in part associated with blood vessels (Supplementary Figure 3C). Analysis of published single-cell RNA-seq data [27] indicates that genes encoding the various collagen VI subunits are mainly expressed by fibro-adipogenic progenitors, smooth muscle cells and tenocytes (Supplementary Figure 3D). Collectively, these data suggest that C5 marks a subset of fibroblasts/fibro-adipogenic progenitors and blood vessel-associated cells responsible for synthesizing collagen VI. Notably, this pattern is not affected by the loss of the furin-like cleavage site. To further investigate the impact of the furin-like cleavage site mutation, we performed immunoblot analysis of collagen VI composition in muscle lysates from 10-week-old and 1-year-old mice (Fig. 2E,F). A western blot with the collagen VI α1-chain-specific antibody showed similar amounts in both wild type and ΔFurin muscles. Interestingly, probing the same samples with the α3N antibody revealed two distinct molecular weight forms. In wild type muscle, the α3 chain displayed a molecular weight of approximately 200 kDa, corresponding to the fully processed chain. In

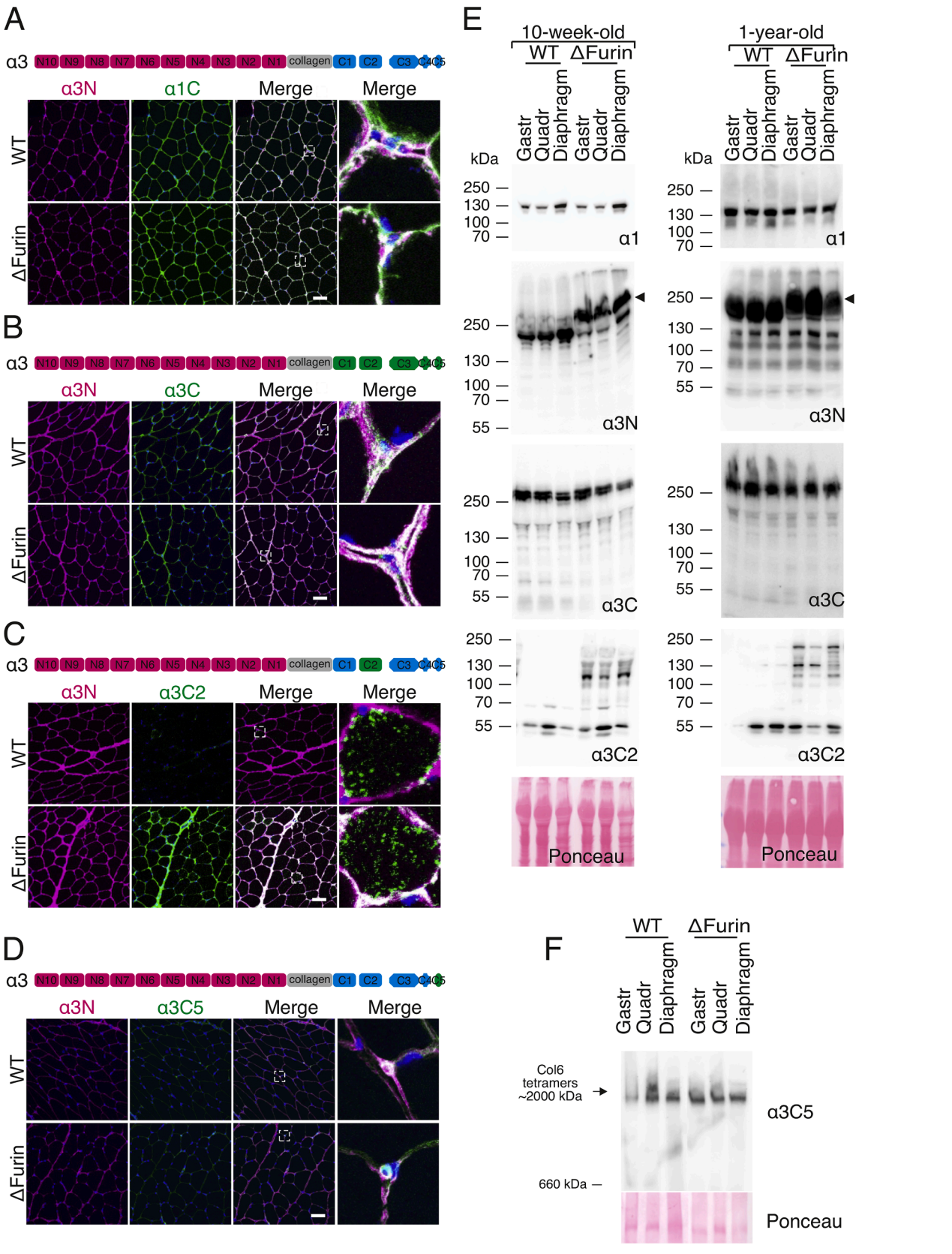

(caption on next page)

Fig. 2. Collagen VI deposition in skeletal muscle is not affected by the ΔFurin mutation despite the presence of different α3 chain species. (**A-D**) Schematic representation of the domain structure of the collagen VI α3 chain. The segment recognized by the α3 N antibody is indicated in *magenta*, while those recognized by the different C-terminal domain specific antibodies are in *green*. Cross sections of quadriceps muscles from 10-week-old wild type (WT) and ΔFurin mice were co-stained with the indicated antibodies. Note that the ubiquitous deposition of collagen VI microfibrils in the interstitial matrix, as revealed by staining with the α3N and α1 or α3C antibodies, was unaffected by the ΔFurin mutation. On the contrary, staining with an antibody specific for the C2 domain of the α3 chain (**C**) revealed a striking difference between wild type and ΔFurin muscles. Note that in the wild type the C2-specific labeling is almost completely lost, with only a few myofibers showing a patchy positive signal, while in ΔFurin sections the labeling overlaps with the α3 N antibody, indicating that in the mutant the C2 domain is not released from the collagen VI microfibrils. C5 was mostly pericellular localized around a few scattered cells that are the *bona fide* collagen VI producing cells in muscle (**D**). The *merged* panels on the right show a 10-fold magnification of the marked area. Scale bars: 50 μm. (**E**) Muscles of 10-week-old and 1-year-old wild type (WT) and ΔFurin mice were lysed and probed with the indicated antibodies under reducing conditions. Notably, using the antibody specific for the N-terminal half of the α3 chain, a slower-migrating band was detected in the ΔFurin muscle (*arrowheads*) compared to wild type. This band may represent tissue accumulation of the non-processed collagen VI α3 chain due to the mutation in ΔFurin mice. Immunoblot with the C2 antibody confirmed the presence of C2 high molecular weight fragments in ΔFurin but not wild type muscle. (**F**) Immunoblot analysis of the same samples under non-reducing conditions in agarose/polyacrylamide composite gels revealed similar levels of C5 domain containing collagen VI tetramers in wild type and ΔFurin muscle.

contrast, the α3N antibody detected a slower-migrating major band in ΔFurin samples, presumably representing the unprocessed α3 chain. Conversely, the α3C (C1-C5) antibody revealed a ~250 kDa band of similar intensity in both wild type and mutant muscles. The most striking difference was observed with the antibody specific to the C2 domain. In wild type muscles, only a signal at around 60 kDa was detected, whereas in ΔFurin samples, a band of ~120 kDa was also evident, most likely representing a C2-C4 fragment that is slowly released by alternative proteases. Densitometric quantification of immunoblots from muscles of different ages confirmed a significant increase in C2-containing species, whereas the α1 and α3C antibodies showed similar signal intensities (Supplementary Figure 4A). Finally,

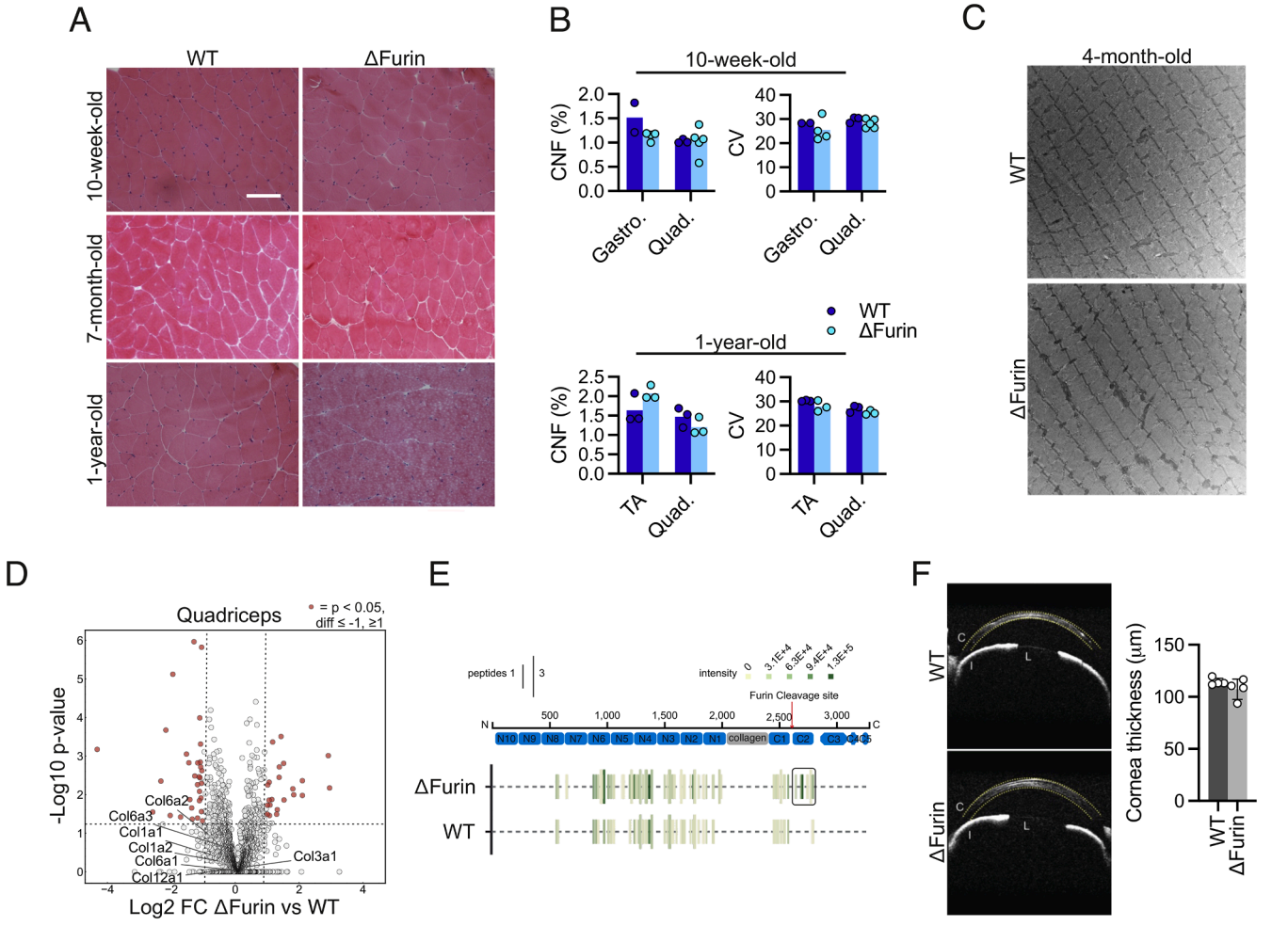

Fig. 3. Inactivation of the furin-cleavage site has no evident consequences in skeletal muscle and cornea. (**A**) Frozen sections of quadriceps muscles of animals of the indicated age were stained with hematoxylin and eosin. Scale bar: 100 μm. (**B**) Centrally nucleated fibers and Feret's minimal diameter were quantified from cross sections for the indicated muscles. Results showed no significant differences. Each data point represents one animal. $N = 2–5$, unpaired *t*-tests. (**C**) Representative electron microscopy micrographs of wild type and ΔFurin quadriceps muscle of 17-week-old mice. (**D**) Volcano plots comparing protein fold changes between ΔFurin and wildtype muscles. Collagen VI chains, as well as other collagens, also showed comparable levels. Labeled proteins are at least twofold regulated and show $P < 0.05$. $n = 6$ per genotype. (**E**) Peptidogram of the peptides and their intensities that were recovered from quadriceps lysates of wild type and ΔFurin muscles. Note that in wild type muscle, the C-terminal part of the α3 chain encompass only the C1 domain, while in the ΔFurin situation, the C2 domain is also retained. The domain structure of the α3 chain is shown on top of the peptidogram for reference. (**F**) Corneal thickness in wild type and ΔFurin mice as assessed by *in vivo* optical coherence tomography. Each data point represents one animal. No statistical difference. Unpaired *t*-test. C: cornea; I: iris; L: lens.

probing the muscle lysates with the C5 antibody aiming at characterizing the C5-containing collagen VI species did not reveal a significant presence of C5-containing fragments in either wild type or ΔFurin muscle lysates (data not shown). However, when the same samples were analyzed on agarose-polyacrylamide composite gels, collagen VI tetramers migrating at the expected molecular weight of ~2000 kDa were equally detected with the C5 antibody in both wild type and ΔFurin muscles (Fig. 2F). This suggests that these tetramers may represent a pool of newly synthesized collagen VI, for which proteolytic processing has not yet occurred, and that collagen VI tetramers are formed at a similar rate in both wild type and ΔFurin muscles.

The loss of the collagen VI α3 chain furin-like cleavage site has no obvious consequences in skeletal muscle and cornea

To evaluate the impact of the ΔFurin mutation on collagen VI function in skeletal muscle, we conducted morphometric and histological analyses on various mouse muscles at different ages. Histological examination did not reveal any evident differences between the two genotypes. Muscle weight in ΔFurin mice was comparable to that of wild type mice at one year of age (Supplementary Figure 1C). We then measured the fraction of centrally nucleated fibers and the minimal Feret's diameter in wild type and ΔFurin mice at two months and one year of age. Previous studies have shown that these parameters are altered in collagen VI-deficient muscle [28,29]. However, in ΔFurin muscle, we observed no significant differences at either time point (Fig. 3B).

Transmission electron microscopy images did not reveal any significant differences between wild type and ΔFurin muscles (Fig. 3C). Mass spectrometry analysis likewise confirmed comparable amounts of collagen VI and other collagens in mutant quadriceps muscle (Fig. 3D, Supplementary Figure 4B and Supplementary Table 1). In summary, the absence of the furin-like cleavage site did not significantly affect collagen VI's role in maintaining normal muscle homeostasis under basal conditions.

Nevertheless, a mass spectrometry-derived peptidogram (Fig. 3E) clearly demonstrated that in wild type muscle, the C-terminal portion of the α3 chain is completely absent, with only peptides derived N-terminal of the C1 domain detected, indicating that domains of the collagen VI α3 chain C-terminal of the furin cleavage site are absent in tissues under

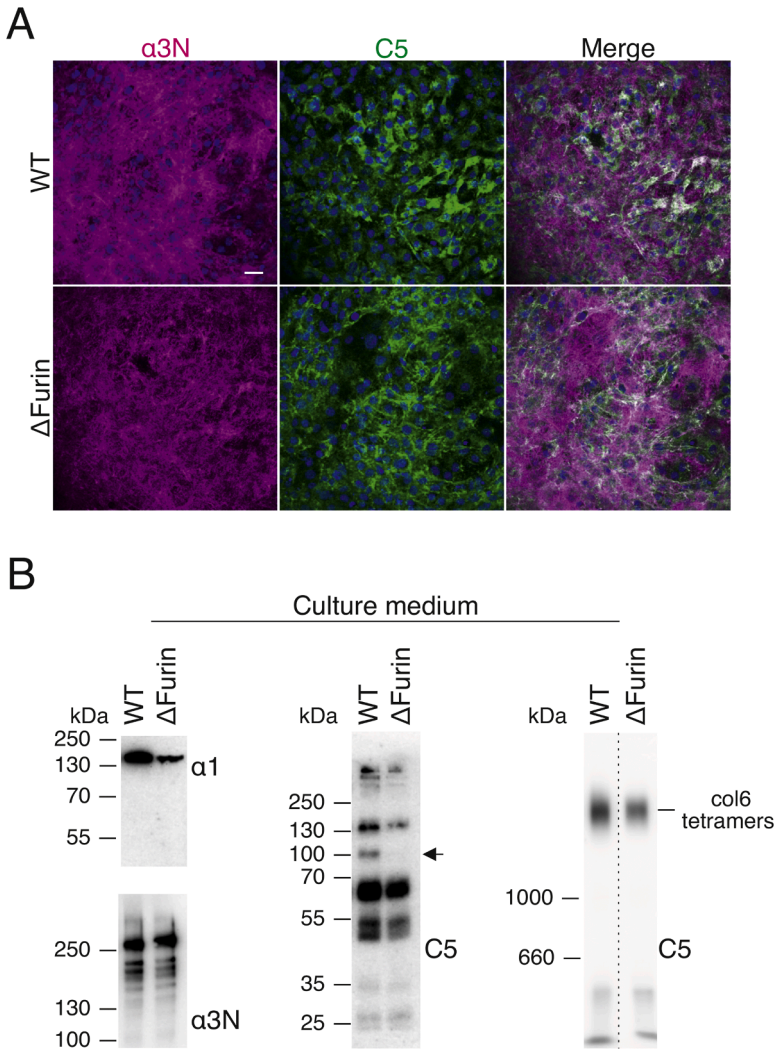

Fig. 4. The ΔFurin mutation has no impact on collagen VI fibril assembly and processing in muscle fibroblasts. (A) Images depict wild type (WT) and ΔFurin immortalized murine muscle fibroblast cultures stained with the designated antibodies. The cells were cultured on glass coverslips, and after reaching confluency, were grown for another four days in complete medium with added ascorbate to induce collagen production. Notice the fibrillar structures labeled with the α3N antibody, while C5 staining was predominantly intracellular. Scale bar: 20 μm. (**B**) Immunoblots of conditioned media from WT and ΔFurin muscle fibroblasts. The cells reached confluency in complete growth medium, were supplemented with ascorbate for two days, and then transferred to serum-free medium with added ascorbate for another two days. The resulting conditioned media were subjected to SDS-PAGE analysis under reducing conditions (α1, α3 N) and non-reducing conditions (C5). For the detection of collagen VI tetramers, an agarose/polyacrylamide composite gel was used.

normal conditions. In contrast, in ΔFurin muscle, not only the C1 domain but also the C2 domain could be detected. However, other domains from the C-terminal region were absent, suggesting that other proteolytic cleavage occurred in the absence of the furin-like cleavage site. This is consistent with the biochemical and immunofluorescence data presented here, which clearly showed that C5 is similarly less abundant in both mouse strains and clearly detectable only with a restricted localization (Fig. 2D).

Collagen VI is a major component of the cornea [30], where we have observed a unique pattern of α3 chain C-terminal processing [14] and no C2-C5 fragment could be detected [22]. However, optical coherence tomography analysis showed that the cornea thickness of 4-month-old ΔFurin mice was comparable to the one of wild type mice (Fig. 3F).

In conclusion, despite the altered composition of collagen VI in wild type and ΔFurin muscle, the absence of the furin-like cleavage site did not significantly affect collagen VI function in maintaining normal muscle and cornea tissue homeostasis under physiological conditions.

Proteolytic processing of the collagen VI α3 chain is not grossly affected by inactivation of the furin-like cleavage site

To further analyze collagen VI processing, we isolated and immortalized fibroblasts from muscle of wild type and ΔFurin newborn mice. Immunofluorescence of the extracellular matrix produced by these fibroblasts after 5 days revealed a dense network of collagen VI microfibrils in both cell lines, detected with the α3N antibodies (Fig. 4A). Co-labeling with the C5 antibody showed mostly intracellular staining in both wild type and ΔFurin fibroblasts (Fig. 4A), consistent with previous reports [31,32]. Next, we analyzed the processing of the α3 chain of collagen VI by immunoblotting the culture media from the same fibroblasts (Fig. 4B). The α3 N antibody primarily labeled high-molecular-weight material corresponding to full-length α3 chain species. Interestingly, a series of faster-migrating bands was also detected, probably representing multiple proteolytically processed species. The C5 antibody similarly revealed a broad range of bands (Fig. 4B), as previously described [4]. Among the C5-positive bands, a 100 kDa band was absent in ΔFurin samples, presumably representing a

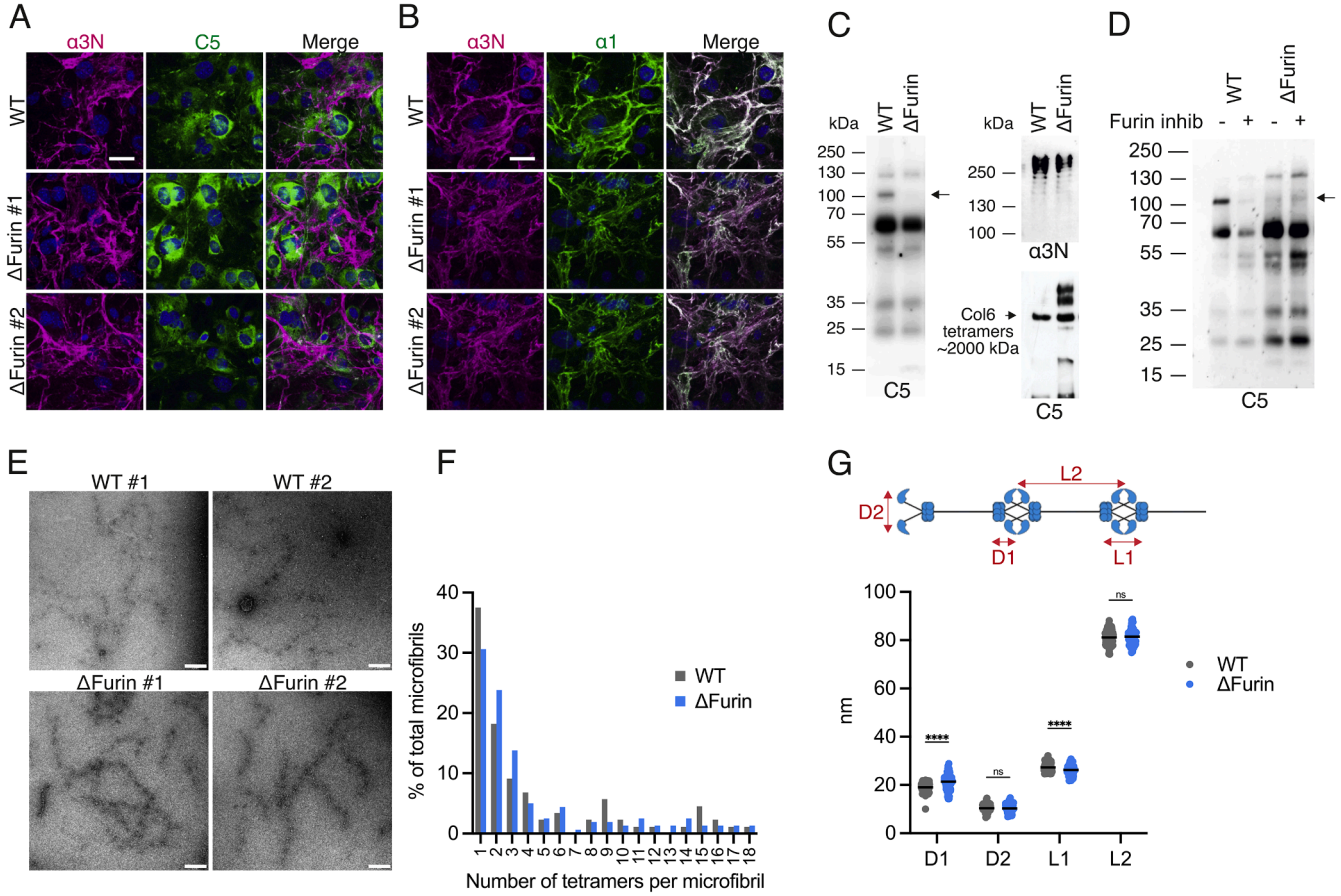

Fig. 5. Effect of the ΔFurin mutation on fibril assembly of collagen VI and processing of the α3 chain in dermal fibroblasts. (**A, B**) Representative images of wild type (WT) and ΔFurin murine primary dermal fibroblast cultures stained with the indicated antibodies. The cells were plated on glass coverslips and grown for four more days after reaching confluency in complete medium supplemented with ascorbate to induce collagen production. Note that both the collagen VI α3N and α1 specific antibodies labeled extracellular fibrils while the C5 specific antibody stained mostly intracellular structures, indicating that the C5 domain is not present in the microfibrils assembled by the fibroblasts. Neither the fibrillar nor the intracellular staining patterns was affected by the ΔFurin mutation. Scale bars: 50 μm. (**C**) Immunoblots of conditioned media from WT and ΔFurin dermal fibroblasts. The cells were grown to confluency in complete growth medium, supplemented with ascorbate for two days, and then switched to serum-free medium plus ascorbate for two more days. The resulting conditioned media were used for SDS-PAGE analysis under reducing (α3N) and non-reducing (C5) conditions. An arrow points to the ~100 kDa C5-positive band that presumably corresponds to the C2-C5 fragment of the α3 chain generated by furin cleavage. For the detection of collagen VI tetramers with the C5 antibody, agarose-acrylamide composite gels were used. (**D**) Immunoblots of conditioned media from wild type (WT) and ΔFurin dermal fibroblasts that were left untreated or treated with 30 μM furin inhibitor for 48 hours. (**E**) Representative images of collagen VI microfibrils in supernatants of wild type (WT) and ΔFurin primary dermal fibroblast cultures visualized by electron microscopy after negative staining. The microfibrils have a similar appearance in the two genotypes. Scale bar: 200 nm. (**F**) Quantitative analysis of collagen VI tetramer-tetramer association. (**G**) Schematic diagram of collagen VI microfibril architecture with highlights of the measured regions. Note the significantly increased size of the globular regions (D1) in the ΔFurin microfibrils. 100 molecules were measured. ns: non significant. Unpaired *t*-tests.

fragment corresponding to C2-C5 [4]. However, other proteolytic products, particularly a prominent 60 kDa band, were equally present in both wild type and ΔFurin samples. Despite numerous attempts, we could only detect very faint bands corresponding to the cleaved-off C5 domain with an expected molecular weight 10 kDa (not shown), suggesting that free C5 constitutes a negligible fraction of C5-containing fragments released by the cells, consistent with prior observations [14]. Composite agarose-polyacrylamide gels confirmed that ΔFurin fibroblasts form and secrete collagen VI tetramers similarly to wild type cells. Moreover, the presence of C5-positive collagen VI tetramers in the culture media of both fibroblast lines supports the notion that α3 chain proteolytic processing occurs, at least partially, extracellularly (Fig. 4B) [4]. We also established primary dermal fibroblast cultures and performed analogous experiments, obtaining results similar to those obtained by using immortalized fibroblasts (Fig. 5A-C). Treatment of these cultures with a furin inhibitor confirmed the identity of the furin-generated 100 kDa C2-C5 band detected with the C5 antibody (Fig. 5D).

Furthermore, electron microscopy after negative staining of collagen VI microfibrils from the conditioned media revealed overall similar structures in wild type and ΔFurin samples (Fig. 5E). Interestingly however, upon closer examination and quantification, WT samples contained a higher relative number of single tetramers and less double and triple tetramers than the Δfurin samples. In ΔFurin microfibrils the globular part of the half beads was less compact in the direction of the extending microfibril than in the wild type ones, and the distance between the globular beads is shorter in ΔFurin than in WT microfibrils, indicating that the changes in the processing of the C-terminus α3 chain of collagen VI have a subtle but distinct effect on the architecture of the globular parts of the microfibrils (Fig. 5F,G).

Altogether, these results demonstrate that multiple proteolytic events occur in the C-terminal part of the α3 chain, and that these events can mostly compensate for the absence of the furin-like cleavage site, leading to a processed form of the chain.

C-terminal fragments of the collagen VI α3-chain do not affect C2C12 myoblast behavior and differentiation

Previous studies have suggested a signaling role for the C5 domain (endotrophin). Our data indicate that C5 is primarily released in larger fragments, including the C2-C5 fragment generated by the furin-like cleavage site (this work and [14]). Additionally, our results suggest that a portion of these fragments may be associated with myofibrils in skeletal muscle (see Figs. 2C and E). Therefore, we studied the bioactivity of these fragments using C2C12 myoblasts as a simplified cellular model of myogenic cells. We recombinantly expressed and purified the C2-C5 fragment and the C5 domain of the murine α3 chain (Fig. 6A). First, we tested the ability of the cells to interact with these proteins by conducting cell attachment and spreading assays. In both assays, C2C12 cells did not interact with the two collagen VI fragments, whereas they

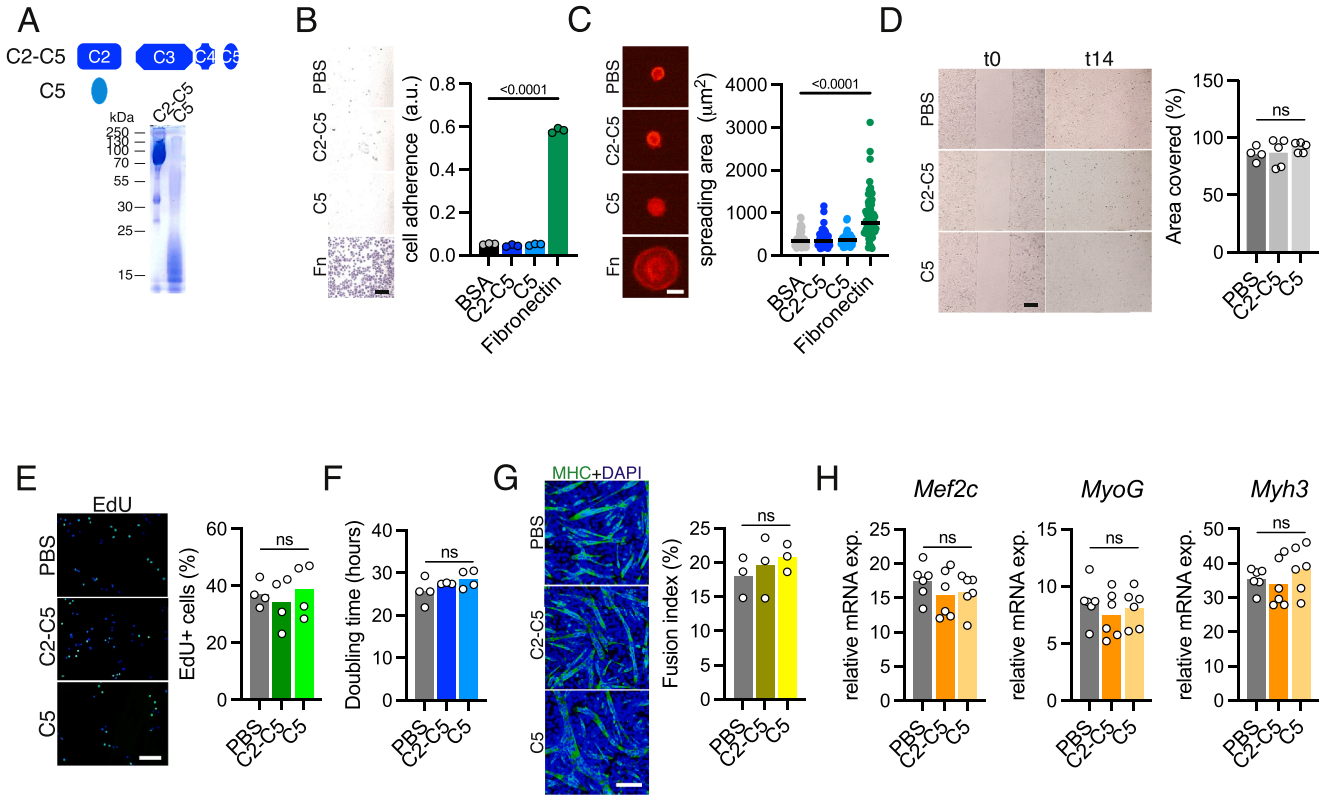

Fig. 6. Bioactivity of fragments derived from the C-terminal part of the α3 chain on C2C12 myoblasts. (**A**) Top: schematic representation of recombinant peptides expressed in HEK293 cells. Below: Coomassie stained SDS polyacrylamide gel of the proteins that were used for the experiments presented in this figure. (**B**) Representative micrographs and quantification of C2C12 cell attachment on surfaces coated with the indicated proteins. Cells attached on fibronectin coated dishes, but not on C2-C5 or C5. Scale bar: 100 μm (**C**) Cell spreading of C2C12 cells on dishes coated with the indicated proteins. C2-C5 and C5 did not support cell spreading, but fibronectin did. Scale bar: 10 μm (**D**) Scratch wound healing assay of C2C12 cells in the presence of C2-C5 or C5 soluble fragments at a concentration of 5 μg/ml. PBS was used as a control. Quantification of the area covered by cells after 14 hours. $n = 4–5$. Scale bar: 200 μm (**E**) Representative images of EdU incorporation in C2C12 myoblasts treated with soluble recombinant proteins at a concentration of 5 μg/ml. The bar chart on the right shows the quantification of the different conditions. (**F**) Cell population doubling time of C2C12 myoblasts grown with 5 μg/ml of the indicated soluble proteins supplemented in the medium. Scale bar: 100 μm (**G**) C2C12 differentiated for two days in low-serum medium in the presence of the indicated soluble fragments. PBS was added as a control. Cells were stained for myosin heavy chain (MHC) and the fusion index was calculated as the ratio between the number of nuclei contained in the myotubes and the total nuclei. Scale bar: 100 μm (**H**) RT-qPCR analysis for the indicated transcripts of cells treated as in G. All comparisons are with uncorrected one-way ANOVA tests.

showed robust attachment and spreading on fibronectin (Fig. 6B,C). C2-C5 and C5 fragments also did not affect C2C12 migration in a scratch wound healing assay (Fig. 6D). Next, we evaluated the potential of C2-C5 and C5 proteins to influence cell proliferation; however, EdU incorporation and cell population doubling time did not show any differences (Fig. 6E,F). Finally, we investigated whether the two proteins could alter the myogenic potential of C2C12 cells. C2C12 cells induced to differentiate for four days in low serum medium in the presence of soluble proteins differentiated into myotubes in a similar manner as untreated cells as shown by their fusion index and comparable expression of differentiation markers assessed by RT-qPCR (Fig. 6G and H and Supplementary Figure 5).

Discussion

Collagens undergo extracellular N- and C-terminal processing during maturation and the role of proteases involved (*e.g.* BMP1, ADAMTS family members and meprins) has been studied in detail for fibrillar collagens [33–35]. Also, during maturation of the microfibril forming collagen VI a substantial processing occurs. However, this is limited to the C-terminal globular part of the α3 chain, as it was reported that collagen VI purified from bovine corneal tissue lacks the C2-C5 domains encompassing 75 % of the C-terminal globular part [22,36]. Indeed, a conserved furin-like cleavage consensus site located between the C1 and the C2 domain of the α3 chain was proposed to be involved [14]. Furin-like proprotein convertases can cleave their substrates either in the secretory pathway, at the cell surface or in the extracellular space [37]. Direct involvement of furin-like proprotein convertases in the maturation of collagen V was already proposed [38,39]. Therefore, we studied in detail the functional role of the furin-like proprotein convertase cleavage in the α3 chain for collagen VI assembly and function by combining *in vitro* experiments with a mouse model carrying a mutated cleavage site.

Propeptides in fibrillar collagens and in the microfibrillar collagen VI have somewhat different functions. During fibrillar collagen maturation the N- and C-terminal propeptides prevent the formation of fibrils. Only after extracellular cleavage functional fibrils form [40]. Incomplete processing can have severe consequences, as *e.g.* a lack of BMP1 can lead to osteogenesis imperfecta [41]. In contrast, during collagen VI microfibril formation the C-terminal globular part of the α3 chain, in particular the C5 domain, is required for the assembly of the secreted tetramers to microfibrils [21]. It was proposed that only after formation of microfibrils the large C-terminal region of the α3 chain is cleaved off and presents in a broad range of fragments of different size indicating that more cleavage sites exist [14]. However, one of the most prominent is the furin-like proprotein convertase cleavage site that defines the border between mature and immature tetrameric building blocks of collagen VI [22,36]. As could be assumed from earlier work, our results clearly demonstrate that the proprotein convertase–mediated processing is not required for collagen VI assembly into tetramers or for microfibril formation. However, although the composition of the mature microfibrils is different in ΔFurin mice, the mutant animals do not display any obvious phenotype.

In muscle sections (Fig. 2A-D) from wild type and ΔFurin mice stained with antibodies against mature collagen VI epitopes, a strong and uniform staining in the endomysium and perimysium is present, although staining with a C2 specific antibody is overlapping in ΔFurin and lacking in wild type muscles. Also, at the ultrastructural level the muscles of ΔFurin mice do not show obvious abnormalities. Moreover, electron microscopy of collagen VI tetramers and microfibrils in supernatants from ΔFurin and wild type cell cultures revealed only minor differences.

A high-resolution cryoEM structure for collagen VI was recentlypublished [15] and places the C1 domains of the α3 chains on top of the beads [42]. Our results are in line with the cryoEM structure, as the cleavage site can be located at the surface of the beads and a projection of the C2-C5 domains away from the beads is possible. Consequently, the cleavage process is most likely independent of other α chains. Indeed, we could demonstrate that the cleavage occurs also when a single α3 chain is expressed.

The presumable protrusion of the C-terminal domain away from the beads also explains why further proteolytic processing occurs even when the furin-like cleavage site is lost. It remains unclear why the C2–C5 fragment of the α3 chain undergoes extensive proteolytic processing, and what the functional consequences are. *In vitro*, the full length C2-C5 fragment generated by use of the furin-like cleavage site represents only a minor fraction of all fragments produced. *In vivo*, our findings show that in ΔFurin muscle the C2 domain is retained, whereas the C3–C5 fragment is largely lost, indicating activity at alternative cleavage sites. Importantly, retention of the C2 domain within collagen VI microfibrils does not appear to affect tissue homeostasis in muscle and cornea, though further studies are needed to assess its role in other tissues. To our knowledge, specific functions have not been ascribed to the C2 domain of the α3 chain.

Previous studies have proposed roles for BMP1 [14] and MMP14 [23] in releasing the C5 domain or in sequential processing by MMP2, MMP9, and MMP16 [43]. However, the generation of larger fragments remains unclear. The cleaved off C5 domain (endotrophin) has been reported to be required for microfibril formation, to act as a matrikine and as a biomarker in several disease states, though its tissue distribution is still largely uncharacterized. It is also not yet clear whether fluctuations in circulating endotrophin levels arise from increased proteolytic processing, enhanced collagen VI production, or both. Our data indicate that under normal conditions, endotrophin levels in skeletal muscle are very low, not dependent on the furin-like cleavage site and found associated with collagen VI tetramers, supporting the idea that the C5 domain is released immediately after collagen VI synthesis [44], and quickly removed from the tissue. Therefore, increased proteolysis is unlikely to be the sole cause of elevated circulating endotrophin.

Previous studies have suggested a cell-type-specific function of endotrophin [45], even if potential receptors and relevant signaling pathways are still not fully characterized [11]. Our initial investigation using C2C12 cells revealed that C2-C5 and C5 fragments do not show a relevant biological activity in myoblasts. In conclusion, our study reveals that although furin-like processing is highly active, it is dispensable for the basal assembly and function of collagen VI in skeletal muscle.

More studies will be needed to exclude a role for the furin-like cleavage site under specific conditions (for example fibrosis or muscle regeneration) and in other tissues.

Material and methods

Mouse genome editing

Col6α3-ΔFurin mice (C57BL/6N—Col6a3^{em434Cecad}/Cecad) were generated by CRISPR/Cas9 genome editing as described [46]. For this purpose, the DNA sequence coding for arginine 2606 and arginine 2607 of Col6a3 (ENSMUSG00000048126) transcript ENSMUST00000056925 was genetically engineered to encode alanine. 4 μM Alt-RTM guide RNA (5′- GCCTTCCTTCAGGGACCGGA −3′) and 10 μM standard desalted Ultramer™ single-stranded DNA repair template (5′- ATTTCTTCATCT-CATTGAACTGGAACAGTGTGGTAGCCTCTGAGCTGTCCAA-GATGAAAGCCAGGTCTATGTCCA-CATCACTGCCTGCTGCAGCGGCGTCCCTGAAGGAAGGCCTC-CAGCTGCCGAAGCCACA −3′) were electroporated with 4 μM Alt-RTM SpCas9 protein in mouse strain C57BL/6NRj zygotes. CRISPR reagents were purchased from Integrated DNA Technologies (USA) and animals obtained from Janvier Labs (France). Embryos were cultured *in vitro* and transferred to recipients as described [47]. Correct integration of the mutation in the resulting F0 mice was validated by Sanger sequencing of a purified PCR amplicon in the founder as well as the F1 mice. Genome

editing was performed at the *in vivo* Research Facility of the CECAD Research Center, University of Cologne, Germany.

Animals

Mice were bred in C57BL/6 N background and housed in individual ventilated cages in the animal facility of the CECAD Research Center of the University of Cologne, free of pathogens and opportunistic agents according to FELASA recommendations. Health status was monitored quarterly [48] at 22 °C (± 2 °C) and a humidity of 55 % (± 5 %) under 12 h light cycle. Mice were supplied with a standard maintenance diet (V1154, Ssniff Spezialdiaeten GmbH, Germany) and tap water *ad libitum*. All study protocols and experiment procedures were in compliance European, national and institutional guidelines and approved by the competent authority of North-Rhine Westphalia (LANUV NRW, Recklinghausen, Germany). For genotyping of adult mice, ear biopsies were incubated in 300 µL lysis buffer (10 mM Tris, 100 mM EDTA, 0.5 % SDS, pH 8.0) and 10 µL proteinase K (Qiagen, Hilden, Germany), at 55 °C overnight. The DNA was then precipitated with isopropanol, centrifuged for 10 min at 12,000 × *g* at 4 °C, and the pellet washed with 70 % ethanol. The DNA pellet was air dried and then dissolved in 50 µL of 5 mM Tris at pH 8.5. For this purpose, the samples were placed in a heated shaking incubator for at least 2 h. One microliter of the DNA sample was used for the genotyping PCR using the following primers: 5`-AATTGGGACACTGCTGGGAC-3` (forward) and 5`-TGAAGTTGGGTCATCCTCCG-3` (reverse). The PCR product was then digested for 2 h at 37 °C with PstI and the resulting fragments analyzed by agarose gel electrophoresis.

Cell culture

Primary murine dermal and muscle fibroblasts were used in this study. Cells were cultured at 37 °C in complete cell culture medium (DMEM, high glucose, ThermoFisher, Cat#10,566,016 supplemented with 10 % fetal bovine serum (Gibco), 100 U/ml Penicillin, 100 µg/ml Streptomycin (Gibco), 50 µg/ml sodium ascorbate (Sigma-Aldrich) and with 5 % CO_2 if not indicated specifically. Murine dermal fibroblasts were isolated from newborn mice as previously described [49]. Briefly, the torsos of 3-day old mice were disinfected with 70 % ethanol. The torso skin was removed and incubated by floating on trypsin-EDTA overnight at 4 °C with the epidermis facing upwards. The dermis was separated from the epidermis by forceps, minced and incubated with DMEM containing 400 U/ml of collagenase I (Invitrogen) for 1 h at 37 °C. To inhibit furin-like proprotein convertases, dermal fibroblasts were treated with 30 µM furin inhibitor I (Merck Millipore) or DMSO as a control. Muscle fibroblasts were obtained from hindlimb muscles of P7 mice. The muscles from three individual mice per genotype were isolated, pooled together and digested with 100U/mL collagenase II (Worthington) and 2U/mL dispase II (Roche) in complete cell culture medium. After 40 min digestion at 37 °C, the medium was filtered first through a 100 µm cell strainer and centrifuged for 5 min at 400 × g. After centrifugation, the supernatant was discarded and the cell pellet was resuspended in complete medium, filtered through a 40 µm cell strainer and then centrifuged again at 400 × g for 5 min. The supernatant was again discarded and the pellet resuspended in complete medium and plated for expansion culture. For immortalization, fibroblasts were infected with retroviral particles generated in Phoenix amphotropic cells (ATCC CRL-3213) transfected with the pBABE-puro-SV40LT plasmid (Addgene #13,970).

C2C12 myoblasts (ATCC) were grown in DMEM, high glucose (Gibco) supplemented with 10 % fetal bovine serum (Gibco), 100 U/ml Penicillin and 100 µg/ml Streptomycin (Gibco). To induce differentiation, cells were shifted into DMEM supplemented with 2 % horse serum (Gibco) and the medium changed every other day.

Histology and immunohistochemistry

Muscles from 10-weeks, 7-months and 1-year-old wild type and ΔFurin mice were dissected, immediately snap-frozen in cold isopentane and stored at −80 °C until sectioning. Sectioning of samples was carried out in a cryostat (Leica) at a thickness of 7 µm and sections captured with Superfrost Plus adhesive microscopy slides (Carl Roth). Hematoxylin-Eosin staining was performed according to standard methods. For immunostaining, slides were fixed for 10 min with a methanol/acetone solution at −20 °C, blocked for one hour with 1 % FCS in PBS and incubated with the primary antibodies in the same solution overnight at 4 °C or for two hours at room temperature. Next, secondary antibodies and DAPI were applied to sections and these incubated at room temperature for one hour. Slides were then washed in PBS 3 times and mounted with DAKO medium. For immunostaining of cell culture monolayers, 5×10^4 cells were seeded on glass cover slips and grown for 7–14 days and fresh medium with ascorbate added every second day and then fixed an ice-cold methanol/acetone solution at − 20 °C for 10 min. Images were acquired with a Leica SP5 confocal microscope. The following in-house-generated primary antibodies against collagen VI were used: polyclonal rabbit anti α1C and polyclonal rabbit anti α3C [50], polyclonal guinea-pig antibody against α3 N [5], polyclonal rabbit α3C5 [14] and anti α3C2 (this study) (Supplementary Figure 6). Other antibodies used were: goat polyclonal anti collagen IV (Merck AB769), rabbit polyclonal anti nidogen-1 [51], ER-TR7 (Santa Cruz Biotechnology).

Cloning and expression of recombinant proteins and affinity purification of a α3C2 specific antiserum

Full-length wild type collagen VI α1, α2 and α3 chains were cloned from mouse embryonic cDNA using the following primers: col6α1: 5′ CAATGCTAGCACAGGACATCCAGGGCTC-3′ and 5′-CAATCTCGAGGCCCAGTGCCACCTTC-3′; col6α2: 5′-CAATGCTAGCCCAGCAGCAGGAAGCCATC-3′ and 5′-CAATGGATCCACAGATCCAGCGGATGAAC-3′; col6α3: 5′-CAATGCTAGCCTCAGCTGACATTATTTTCCTTATTG-3′ and 5′-GAATG CGGCCGCAACTGTTAACTCAGGACTACACATC-3′.

The cDNA coding for the C2 domain of the α3 chain was cloned using the following primers: 5′-CAATGCTAGCAGCAGGCAGTGATGTG-3′ and 5′-CAATGCGGCCGCGCTGACAAAGGATGGGAG-3′. Cloning of the C2-C5 and C5 fragments of the α3 chain was previously described [11,14]. A ΔFurin cleavage site version of the α3 chain was generated by PCR using the following primers: 5′-GAGGCCTTCCTTCAGGGACGCTGCT GCAGCAGGCAGTGATGTGGAC-3′ and 5′-GTCCACATCACTGCC TGCTGCAGCAGCGTCCCTGAAGGAAGGCCTC-3′ and assembled using the NEBuilder® HiFi DNA Assembly (New England Biolabs). All the constructs were cloned into sleeping beauty transposase based vectors and sequenced as described before [52]. Expression and purification of recombinant proteins was performed as previously described [11]. Briefly, HEK293-EBNA cells were transfected with FuGENE HD (Promega) and selected with 3 µg/ml puromycin to generate stable lines. Conditioned media were collected for 2–5 days and the recombinant proteins purified on a Strep-Tactin®XT resin (IBA Lifescience), following the manufacturer instructions.

The purified recombinant α3C2 domain was coupled to CNBr-activated Sepharose (Amersham Bioscience). The α3C2 specific antiserum was obtained by affinity chromatography of the polyclonal rabbit anti α3C antiserum [50]. The α3C2 specific antibody, was eluted with 3 M KSCN in TBS and then dialyzed against TBS.

Mass spectrometry

Intact tissue sample processing

Gastrocnemius muscles were extracted and snap frozen, lyophilized and lysed in 4 % SDS in PBS. The tissue lysate was heated to 95 °C and sonicated using the Bioruptor sonicator. The supernatant was collected

after centrifugation at 18,000 *g* for 10 min. 10 μg of the protein extract was reduced and alkylated for 10 min at 75 °C using 5 mM TCEP and 15 mM CAA. Protein digestion was performed following the SP3 protocol [53]. Proteins were digested with trypsin and LysC overnight at 37 °C. Digested peptides were acidified to 0.1 % formic acid (FA) and cleaned-up using house-made SDB-RPS tips.

For further downstream LC-MS/MS analysis, the desalted peptides were measured on a EvoSep one HPLC system (EvoSep, Denmark) coupled to timsTOF pro2 using a CaptiveSpray source (Bruker, USA). Peptide separation was performed with a gradient length of 44 min (30 SPD) with the HPLC system equipped with 15 cm PepSep columns (EvoSep, Denmark) at 30 °C column temperature. The ionized peptides were measured in dia-PASEF mode with window sizes ranging in dimension 1/k0 0.7–1.35, with 24 × 25 Th and in dimension *m/z* from 400 to 1000. Spectra were analyzed with a library free search against the UniProt mouse database (2023) using DIA-NN 1.8.1. Data input was filtered for unique peptides, q-Value ⟨0.01, Lib.Q.Value <0.01, PG.Q. Value < 0.01, Global.Q.Value < 0.01, Quantity.Quality ⟩ 0.7, Fragment. count ≥ 4. Welchs *t*-test corrected for multiple comparisons was performed with Perseus (V.1.6.5.0) and further visualization with Instant clue (V 0.10.10.20210315).

In-gel digest

For In-gel digest samples, each lane from the SDS-PAGE gel were excised into 4–5 equal parts and further shredded into smaller pieces and destained with Acetonitrile. The samples were reduced and alkylated with DTT (10 mM) and CAA (55 mM) respectively. Proteins were digested with 3 ng of Trypsin and LysC in 50 mM TEAB at 37 °C overnight. Samples were acidified to 0.1 % formic acid (FA) and cleaned-up using house-made SDB-RPS tips.

Reverse phase liquid chromatography of peptides and MS/MS analysis was performed using an Easy nLC 1000 UHPLC coupled to a Orbitrap Eclipse mass spectrometer (Thermo Fischer Scientific, USA). Peptide separation was obtained through a gradient length of 60 min with an in-house made 30 cm column with a fused silica emitter (75 μm-diameter). The MS was operated in a data-dependent mode, with MS1 scans in the range of 375–2000 *m/z*. The 20 most intense peaks ($z \geq 2$) from the MS1 scans were selected and fragmented in the high-energy collision induced dissociation (HCD) cell and MS2 spectra were recorded. Spectra were analyzed using library free search against the UniProt mouse database (2023) with MaxQuant 2.2.0 with parent and fragment mass tolerances set at 20 ppm and 4.5 ppm respectively and PSM and protein FDR set at 1 %. Maximum missed cleavages were set at 2 with a minimum peptide length of 7 and maximum of 25 with a peptide charge state of 2 Carboamidomethylation of cysteine residues was searched for as fixed modification N-terminal acetylation and oxidation of methionines was looked for as variable modifications. Further Statistical analysis was performed with Perseus (V.1.6.5.0) and visualized with Instant clue (V 0.10.10.20210315).

Assessment of mean corneal thickness (MCT)

Mean corneal thickness (MCT) was measured using volumetric scans of the anterior segment obtained through *in vivo* optical coherence tomography (OCT) with the Telesto OCT System (Thorlabs, Lübeck, Germany), following a previously established protocol [54]. Each B-scan comprised a 512 × 512 pixel resolution, covering an area of 2.5 mm by 2.5 mm with a depth of 1.87 mm. Spatial resolution was calculated based on the corneal refractive index (1.376), resulting in scaling factors of 3.65 μm/pixel axially and 4.88 μm/pixel laterally. MATLAB software (The MathWorks, Inc., Natick, MA) was used to analyze corneal thickness. OCT scan volumes were imported into MATLAB and segmented into ten frame stacks. A maximum intensity projection (MIP) image was generated for each stack. The lens was identified using a multi-threshold algorithm and subsequently excluded. After enhancing image contrast and applying a median filter, Sobel edge detection was used to delineate the anterior and posterior corneal boundaries. Edge gradients were analyzed, and points with extreme derivatives were discarded. Missing edge data was interpolated linearly, with manual adjustments applied as needed. Corneal thickness was calculated as the vertical distance between segmented anterior and posterior edges. Measurements outside two standard deviations from the MIP mean thickness were discarded. The final MCT was determined by averaging thicknesses across all MIP images in the volume.

SDS-polyacrylamide and agarose/polyacrylamide gel electrophoresis and immunoblotting

Tissue was homogenized and extracted with 4 % SDS in PBS, and with Complete protease inhibitor (Roche Diagnostics, Mannheim, Germany). Extracts were subjected to SDS-polyacrylamide gel electrophoresis on 4–12 % or 10 % polyacrylamide gels. Resolved proteins were electrophoretically transferred to a nitrocellulose membrane and loading controlled by Ponceau S staining. The membrane was incubated in 5 % (w/v) milk powder in TBS, for 1 h at room temperature. Primary antibodies were prepared by dilution in 5 % milk powder (w/v) in TBS, and incubated with the membrane for either 1 h at RT or overnight at 4 °C. The membrane was washed three times with TBS containing 0.1 % (v/v) Tween-20 (TBS-T). Secondary antibodies were also diluted again in 5 % milk powder and incubated for 1 h at RT. The membrane was again repeatedly washed, incubated with ECL (Cytiva) solution and imaged using a Cytiva ImageQuant 800 Western blot imaging systems. For the detection of collagen VI tetramers, agarose/polyacrylamide gels were used as in [11].

Electron microscopy

Small muscles samples of 4-month-old mice were fixed in 2 % (v/v) formaldehyde and 2.5 % (v/v) glutaraldehyde in 100 mM cacodylate buffer, pH 7.4, at 4oC overnight. After washing in PBS, samples were postfixed in 0.5 % (v/v) osmium tetroxide and 1 % (w/v) potassium hexacyanoferrate (III) in 0.1 M cacodylate buffer for 2 h at 4oC followed by washing with distilled water. After dehydration in an ascending ethanol series from 30 to 100 % ethanol, specimens were incubated twice in propylene oxide for 15 min each and embedded in Epon using flat embedding molds. Ultrathin sections were cut with an ultramicrotome, collected on copper grids and negatively stained with 2 % uranyl acetate for 10 min. Electron micrographs were taken at 60 kV with a Veleta camera system in combination with the Radius software system (emsis, Münster, Germany).

For negative staining and transmission electron microscopy, aliquots of fibroblast supernatants were directly applied onto copper grids, negatively stained and assessed as follows. Specimen samples were adsorbed to 400-mesh carbon-coated copper grids for 60 s, briefly washed with H2O, and then stained with 0.75 % (w/v) uranyl formate for 60 s. The grids had been rendered hydrophilic by glow discharge at a low pressure in air. Specimens were examined in a Philips/FEI CM 100 TWIN transmission electron microscope at 60 kV accelerating voltage. Microfibril architecture and dimensions were manually analyzed in Photoshop CS6 using the ruler tool.

RT-qPCR

RNA extraction was carried out with TRIzol™ (Invitrogen) following the manufacturer's protocol. Total RNA (1–2 μg per sample) was reverse transcribed using the OmniScript RT Kit (Qiagen). Technical duplicates for every sample were amplified using the Takyon ROX SYBR 2X MasterMix dTTP blue (Eurogentec) either in a StepOnePlusTM real-time PCR detection system (Applied Biosystems) or in a LightCycler 480 (Roche). Data analysis was performed using the $2^{-\Delta\Delta Ct}$ method and quantified relative to *GAPDH*. Primer sequences were: *GAPDH*: 5′-CCACCCAGAAGACTGTGGAT-3′, 5′-TTCAGCTCTGGGATGACCTT-3′;

Myh3: 5′-CGCAGAATCGCAAGTCAATA-3′, 5′-ATATCTTCTGCCCTG-CACCA-3′; *MyoG*: 5′-CTTGCTCAGCTCCCTCAACC-3′, 5′-GTTGGGACC-GAACTCCAGTG-3′; *Mfe2c: 5′-TGATCAGCAGGCAAAGATTG-3′, 5′-ATCAGACCGCCTGTGTTACC-3′.*

EdU and proliferation assay

8×10^4 C2C12 cells were plated on glass coverslips. The next day cells were washed once in PBS and treated with 10 μM EdU for 1 h in DMEM medium containing 2 % fetal bovine serum prior to fixation with 4 % PFA/PBS. The coverslips were then processed using the 488 EdU Click Proliferation Kit (BD Pharmingen) according to the manufacturer's protocol. To assess cell proliferation, 4×10^4 C2C12 cells were plated per well in 48-well plates in 0.5 mL of DMEM with 2 % fetal bovine serum. After 24 hours, cells were washed with PBS and treated with 5 μg/mL recombinant proteins in fresh 2 % FCS medium. Cell growth was monitored using an Omni live-cell imager (Axion Biosystems). Confluency was estimated with the integrated software and population doubling time was finally calculated using the following formula: Doubling Time = $T * \ln(2) / \ln(Xe / Xb)$, where T = time interval for measzrments (=24 h) Xb = initial cell confluency Xe = final cell confluency.

Scratch wound healing assay

C2C12 myoblasts were suspended at 500,000 cells/mL and 70 μL of suspension were seeded on tissue culture plastic in each chamber of culture inserts (Ibidi, cat no. 80,209). Cells were allowed to adhere and reach confluence over 24 hours. Inserts were then removed to create a defined gap, and fresh DMEM with 2 % FCS and recombinant proteins were added. Brightfield images were taken at multiple time points using a EVOS XL Core microscope (Thermo Fisher). Closure of the gap was measured using ImageJ as described [55].

Cell spreading and attachment

For both assays, wells were coated either with 10 μg/mL fibronectin (Sigma), or recombinant C2-C5 or C5 overnight at 4 °C. Wells were then washed with PBS, and blocked with 1 % BSA for 60 min at room temperature. C2C12 myoblasts were detached using trypsin/EDTA, washed twice in serum-free medium (SFM) to remove residual trypsin and FCS, and resuspended in serum free medium before plating.

For the spreading assay, cells were seeded and allowed to adhere for 1 h, washed once in PBS and then fixed in 4 % PFA for 15 min. Cells were permeabilized with 0.5 % NP-40 in PBS for 15 min, followed by staining with fluorescent phalloidin (Cell Signaling) and DAPI.

For the cell attachment assay After 1 h of adhesion, cells were washed three times with SFM, fixed in 4 % PFA for 15 min. Adherent cells were stained with 0.1 % crystal violet in deionized water for 30 min, washed with tap water, let dry and imaged. Attached cells were then lysed and crystal violet staining quantified at 570 nm with a plate reader (Tecan).

C2C12 cell differentiation

$40 \times 10^4/cm^2$ C2C12 myoblasts were seeded in triplicates on glass coverslips. The next day, cells were when indicated supplemented with 5 μg/ml recombinant proteins. After 24 hours, differentiation was induced by replacing the medium to DMEM with 2 % horse serum, with the addition of 5 μg/mL of recombinant proteins. For fusion index analysis, cells after 2 days of differentiation were fixed in ice-cold methanol/acetone (1:1) for 10 min at −20 °C, followed by immunostaining for muscle myosin (mouse monoclonal antibody F59, Santa Cruz), and staining with DAPI. The fusion index was calculated as the number of nuclei inside myosin-positive myotubes divided by the total number of nuclei, counted from at least three random microscopic fields per replicate.

Acknowledgements

We thank Birgit Kobbe for her technical assistance. This research was funded by DFG project ID 384170921 (FOR2722/B1-407164210 to MP and RW), PA660/12-2 (MP), SCHI1627/2-2 (AS), KR3788/8-2 (MKr) and KO2247/8-2 to MK.

Supplementary materials

Supplementary material associated with this article can be found, in the online version, at doi:10.1016/j.matbio.2025.11.003.

Data availability

No data was used for the research described in the article.

References

[1] M. Cescon, F. Gattazzo, P. Chen, P. Bonaldo, Collagen VI at a glance, J. Cell. Sci. 128 (19) (2015) 3525–3531.
[2] C.G. Bönnemann, The collagen VI-related myopathies: muscle meets its matrix, Nat. Rev. Neurol. 7 (7) (2011) 379–390.
[3] S.K. Gara, P. Grumati, A. Urciuolo, P. Bonaldo, B. Kobbe, M. Koch, et al., Three novel collagen VI chains with high homology to the alpha3 chain, J. Biol. Chem. 283 (16) (2008) 10658–10670.
[4] J. Fitzgerald, C. Rich, F.H. Zhou, U. Hansen, Three novel collagen VI chains, alpha4 (VI), alpha5(VI), and alpha6(VI), J. Biol. Chem. 283 (29) (2008) 20170–20180.
[5] S.K. Gara, P. Grumati, S. Squarzoni, P. Sabatelli, A. Urciuolo, P. Bonaldo, et al., Differential and restricted expression of novel collagen VI chains in mouse, Matrix. Biol. 30 (4) (2011) 248–257.
[6] S.R. Lamande, J.F. Bateman, Collagen VI disorders: insights on form and function in the extracellular matrix and beyond, Matrix. Biol. 71-72 (2018) 348–367.
[7] J. Park, P.E. Scherer, Adipocyte-derived endotrophin promotes malignant tumor progression, J. Clin. Invest. 122 (11) (2012) 4243–4256.
[8] J. Wang, W. Pan, The biological role of the collagen alpha-3 (VI) chain and its cleaved C5 domain fragment endotrophin in cancer, Onco Targets. Ther. 13 (2020) 5779–5793.
[9] K. Sun, J. Park, O.T. Gupta, W.L. Holland, P. Auerbach, N. Zhang, et al., Endotrophin triggers adipose tissue fibrosis and metabolic dysfunction, Nat. Commun. 5 (2014) 3485.
[10] D.W. Bu, C. Crewe, C.M. Kusminski, R. Gordillo, A.L. Ghaben, M. Kim, et al., Human endotrophin as a driver of malignant tumor growth, JCI. Insight. 4 (9) (2019).
[11] M. Przyklenk, S.E. Heumuller, C. Freiburg, S. Lutke, G. Sengle, M. Koch, et al., Lack of evidence for a role of anthrax toxin receptors as surface receptors for collagen VI and for its cleaved-off C5 domain/endotrophin, iScience 25 (10) (2022) 105116.
[12] F. Genovese, C. Bager, P. Frederiksen, D. Vazquez, J.M.B. Sand, R.G. Jenkins, et al., The fibroblast hormone endotrophin is a biomarker of mortality in chronic diseases, Matrix. Biol. 132 (2024) 1–9.
[13] K. Henriksen, F. Genovese, A. Reese-Petersen, L.P. Audoly, K. Sun, M.A. Karsdal, et al., Endotrophin, a key marker and driver for fibroinflammatory disease, Endocr. Rev. 45 (3) (2024) 361–378.
[14] S.E. Heumüller, M. Talantikite, M. Napoli, J. Armengaud, M. Mörgelin, U. Hartmann, et al., C-terminal proteolysis of the collagen VI α3 chain by BMP-1 and proprotein convertase(s) releases endotrophin in fragments of different sizes, J. Biol. Chem. 294 (37) (2019) 13769–13780.
[15] A.R.F. Godwin, M.H. Becker, R. Dajani, M. Snee, A.M. Roseman, C. Baldock, Collagen VI microfibril structure reveals mechanism for molecular assembly and clustering of inherited pathogenic mutations, Nat. Commun. 16 (1) (2025) 7549.
[16] C. Knupp, J.M. Squire, A new twist in the collagen story–the type VI segmented supercoil, EMBO J. 20 (3) (2001) 372–376.
[17] S.G. Ball, C. Baldock, C.M. Kielty, C.A. Shuttleworth, The role of the C1 and C2 A-domains in type VI collagen assembly, J. Mol. Biol. 330 (2) (2003) 297–307.
[18] S.G. Ball, J. Bella, C.M. Kielty, C.A. Shuttleworth, Structural basis of type VI collagen dimer formation, J. Biol. Chem. 278 (17) (2003) 15326–15332.
[19] J. Engel, H. Furthmayr, E. Odermatt, H. von der Mark, M. Aumailley, R. Fleischmajer, et al., Structure and macromolecular organization of type VI collagen, Ann. N. Y. Acad. Sci. 460 (1985) 25–37.
[20] C. Baldock, M.J. Sherratt, C.A.A. Shuttleworth, Kielty CM. The supramolecular organization of collagen VI microfibrils, J. Mol. Biol. 330 (2) (2003) 297–307.
[21] S.R. Lamandé, M. Mörgelin, N.E. Adams, C. Selan, J.M. Allen, The C5 domain of the collagen VI alpha3(VI) chain is critical for extracellular microfibril formation and is present in the extracellular matrix of cultured cells, J. Biol. Chem. 281 (24) (2006) 16607–16614.
[22] A. Eckersley, K.T. Mellody, S. Pilkington, C.E.M. Griffiths, R.E.B. Watson, R. O'Cualain, et al., Structural and compositional diversity of fibrillin microfibrils in human tissues, J. Biol. Chem. 293 (14) (2018) 5117–5133.

[23] X. Li, Y.S. Zhao, C. Chen, L. Yang, H.H. Lee, Z.N. Wang, et al., Critical role of matrix metalloproteinase 14 in adipose tissue remodeling during obesity, Mol. Cell. Biol. 40 (8) (2020).
[24] H. Ishikawa, K. Sugie, K. Murayama, A. Awaya, Y. Suzuki, S. Noguchi, et al., Ullrich disease due to deficiency of collagen VI in the sarcolemma, Neurology 62 (4) (2004) 620–623.
[25] A. Schiavinato, M. Przyklenk, B. Kobbe, M. Paulsson, R. Wagener, Collagen type VI is the antigen recognized by the ER-TR7 antibody, Eur. J. Immunol. 51 (9) (2021) 2345–2347.
[26] Y. Zou, R.-Z. Zhang, P. Sabatelli, M.-L. Chu, C.G. Bönnemann, Muscle interstitial fibroblasts are the main source of Collagen VI synthesis in skeletal Muscle: implications for congenital muscular dystrophy types Ullrich and Bethlem, J. Neuropathol. Exp. Neurol. 67 (2) (2008) 144–154.
[27] M.J. Petrany, C.O. Swoboda, C. Sun, K. Chetal, X. Chen, M.T. Weirauch, et al., Single-nucleus RNA-seq identifies transcriptional heterogeneity in multinucleated skeletal myofibers, Nat. Commun. 11 (1) (2020) 6374.
[28] P. Bonaldo, P. Braghetta, M. Zanetti, S. Piccolo, D. Volpin, G.M. Bressan, Collagen VI deficiency induces early onset myopathy in the mouse: an animal model for Bethlem myopathy, Hum. Mol. Genet. 7 (13) (1998) 2135–2140.
[29] P. Mohassel, H. Hearn, J. Rooney, Y. Zou, K. Johnson, G. Norato, et al., Collagen type VI regulates TGF-β bioavailability in skeletal muscle in mice, J. Clin. Invest. 135 (9) (2025).
[30] D.R. Zimmermann, B. Trüeb, K.H. Winterhalter, R. Witmer, R.W. Fischer, Type VI collagen is a major component of the human cornea, FEBS Lett. 197 (1–2) (1986) 55–58.
[31] U. Mayer, E. Poschl, R. Nischt, U. Specks, T.C. Pan, M.L. Chu, et al., Recombinant expression and properties of the Kunitz-type protease-inhibitor module from human type VI collagen alpha 3(VI) chain, Eur. J. Biochem. 225 (2) (1994) 573–580.
[32] T. Aigner, L. Hambach, S. Soder, U. Schlotzer-Schrehardt, E. Poschl, The C5 domain of Col6A3 is cleaved off from the Col6 fibrils immediately after secretion, Biochem. Biophys. Res. Commun. 290 (2) (2002) 743–748.
[33] E. Kessler, K. Takahara, L. Biniaminov, M. Brusel, D.S. Greenspan, Bone morphogenetic protein-1: the type I procollagen C-proteinase, Science 271 (5247) (1996) 360–362.
[34] M. Bekhouche, A. Colige, The procollagen N-proteinases ADAMTS2, 3 and 14 in pathophysiology, Matrix. Biol. 44-46 (2015) 46–53.
[35] J. Prox, P. Arnold, C. Becker-Pauly, Meprin α and meprin β: procollagen proteinases in health and disease, Matrix. Biol. 44-46 (2015) 7–13.
[36] N. Beecher, A.M. Roseman, T.A. Jowitt, R. Berry, H. Troilo, R.A. Kammerer, et al., Collagen VI, conformation of A-domain arrays and microfibril architecture, J. Biol. Chem. 286 (46) (2011) 40266–40275.
[37] N.G. Seidah, A. Prat, The biology and therapeutic targeting of the proprotein convertases, Nat. Rev. Drug Discov. 11 (5) (2012) 367–383.
[38] Y. Imamura, B.M. Steiglitz, D.S. Greenspan, Bone morphogenetic protein-1 processes the NH2-terminal propeptide, and a furin-like proprotein convertase processes the COOH-terminal propeptide of pro-alpha1(V) collagen, J. Biol. Chem. 273 (42) (1998) 27511–27517.
[39] C. Unsöld, W.N. Pappano, Y. Imamura, B.M. Steiglitz, D.S. Greenspan, Biosynthetic processing of the pro-alpha 1(V)2pro-alpha 2(V) collagen heterotrimer by bone morphogenetic protein-1 and furin-like proprotein convertases, J. Biol. Chem. 277 (7) (2002) 5596–5602.
[40] J. Bella, Hulmes DJ.Fibrillar Collagens, SubCell Biochem. 82 (2017) 457–490.
[41] D. Syx, B. Guillemyn, S. Symoens, A.B. Sousa, A. Medeira, M. Whiteford, et al., Defective proteolytic processing of fibrillar procollagens and prodecorin due to biallelic BMP1 mutations results in a severe, progressive form of osteogenesis Imperfecta, J. Bone Miner. Res. 30 (8) (2015) 1445–1456.
[42] A.R. Godwin, T. Starborg, M.J. Sherratt, A.M. Roseman, C. Baldock, Defining the hierarchical organisation of collagen VI microfibrils at nanometre to micrometre length scales, Acta Biomater. 52 (2017) 21–32.
[43] W. Jo, M. Kim, J. Oh, C.S. Kim, C. Park, S. Yoon, et al., MicroRNA-29 ameliorates fibro-inflammation and insulin resistance in HIF1α-deficient obese adipose tissue by inhibiting endotrophin generation, Diabetes 71 (8) (2022) 1746–1762.
[44] T. Aigner, L. Hambach, S. Söder, U. Schlötzer-Schrehardt, E. Pöschl, The C5 domain of Col6A3 is cleaved off from the Col6 fibrils immediately after secretion, Biochem. Biophys. Res. Commun. 290 (2) (2002) 743–748.
[45] Y. Zhao, X. Gu, N. Zhang, M.G. Kolonin, Z. An, K. Sun, Divergent functions of endotrophin on different cell populations in adipose tissue, Am. J. Physiol. Endocrinol. Metab. 311 (6) (2016) E952–EE63.
[46] S.E. Tröder, L.K. Ebert, L. Butt, S. Assenmacher, B. Schermer, B. Zevnik, An optimized electroporation approach for efficient CRISPR/Cas9 genome editing in murine zygotes, PLoS. One 13 (5) (2018) e0196891.
[47] M. Wigger, M. Schneider, A. Feldmann, S. Assenmacher, B. Zevnik, S.E. Tröder, Successful use of HTF as a basal fertilization medium during SEcuRe mouse *in vitro* fertilization, BMC. Res. Notes. 16 (1) (2023) 184.
[48] M. Mähler Convenor, M. Berard, R. Feinstein, A. Gallagher, B. Illgen-Wilcke, K. Pritchett-Corning, et al., FELASA recommendations for the health monitoring of mouse, rat, hamster, guinea pig and rabbit colonies in breeding and experimental units, Lab. Anim. 48 (3) (2014) 178–192.
[49] M. Sawant, F. Wang, J. Koester, A. Niehoff, M.M. Nava, E. Lundgren-Akerlund, et al., Ablation of integrin-mediated cell-collagen communication alleviates fibrosis, Ann. Rheum. Dis. 82 (11) (2023) 1474–1486.
[50] T. Maaß, C.P. Bayley, M. Mörgelin, S. Lettmann, P. Bonaldo, M. Paulsson, et al., Heterogeneity of collagen VI microfibrils: structural analysis of non-collagenous regions, J. Biol. Chem. 291 (10) (2016) 5247–5258.
[51] J.W. Fox, U. Mayer, R. Nischt, M. Aumailley, D. Reinhardt, H. Wiedemann, et al., Recombinant nidogen consists of three globular domains and mediates binding of laminin to collagen type IV, EMBO J. 10 (11) (1991) 3137–3146.
[52] A. Moya-Torres, M. Gupta, F. Heide, N. Krahn, S. Legare, D. Nikodemus, et al., Homogenous overexpression of the extracellular matrix protein netrin-1 in a hollow fiber bioreactor, Appl. Microbiol. Biotechnol. (2021).
[53] C.S. Hughes, S. Moggridge, T. Müller, P.H. Sorensen, G.B. Morin, J. Krijgsveld, Single-pot, solid-phase-enhanced sample preparation for proteomics experiments, Nat. Protoc. 14 (1) (2019) 68–85.
[54] K. Hadrian, G. Musial, A. Schönberg, T. Georgiev, C. Küper, F. Bock, et al., The role of the osmosensitive transcription factor NFAT5 in corneal edema resorption after injury, Exp. Mol. Med. 55 (3) (2023) 565–573.
[55] A. Suarez-Arnedo, F. Torres Figueroa, C. Clavijo, P. Arbeláez, J.C. Cruz, Muñoz-Camargo C. An image J plugin for the high throughput image analysis of *in vitro* scratch wound healing assays, PLoS. One 15 (7) (2020) e0232565.